Dimensionality Control and Magnetism of Fe on Nanopatterned Au(111) Surface

Wen-Chin Lin[1], Hung-Yu Chang[2], Yu-Cheng Hu[2], and Chien-Cheng Kuo[2,3]

[1]Department of Physics, National Taiwan Normal University, Taipei 11677, Taiwan
[2]Department of Physics, National Sun Yat-sen University, Kaohsiung 80424, Taiwan
[3]Center for Nanoscience and Nanotechnoloy, National Sun Yat-sen University, Kaohsiung 80424, Taiwan

Scanning tunneling microscope (STM) is used to explore the room-temperature (RT) growth and multistep growth of Fe on Au(111) herringbone surface. The statistical analysis of island size and arrangement, combined with a phenomenological magnetic anisotropy energy (MAE) model, can describe the previously reported magnetic behavior of Fe two-dimensional (2-D) island array very well. While increasing the Fe coverage, MAE is dominated by edge atoms, surface atoms, and then shape MAE, sequentially. The multistep growth, combing nucleation seeds, Xe buffer layer, and annealing treatment, reveals the possibility for manipulating the Fe growth into desired multilayer islands.

***Index Terms*—Nanomagnetism, nanostructure, self-assembly.**

I. Introduction

THE studies of nanopatterned templates attracted much attention in the last decade, because of the promising capability for preparation of well-arranged nanodots. For example, the mask effect induced by N/Cu(100) [1], [2], dislocation network of two monoatimic layer (ML) Ag/Pt(111) [3], [4], and Au(111) herringbone reconstruction are highlighted. [5]–[10] In these cases, the well-ordered nucleation sites gradually form two-dimensional (2-D) islands (only one atomic height) and then evolve into thin films with increasing coverage. These 2-D island arrays are of great interests, especially in magnetism, due to the significant contribution from the edge atoms. Some previous studies reveal that the atoms at island edge even dominate the collective magnetic behavior, providing the capability of engineering the magnetic properties of nanoislands [11]. Thus, the detailed 2-D island growth evolution and its corresponding magnetic behavior is carefully characterized and discussed in this paper.

Besides, the natural limitation of 2-D islands on the nanopatterned surface might restrict the functions for the further applications, because controlling of island height is very possibly required to enhance Curie temperature or to modify the magnetic anisotropy [12]–[16]. It is of the importance to study the evolution for the three-dimensional (3-D) and 2-D nanostructures and the corresponding magnetic properties since the dimensionality of the magnetic materials becomes significant while the size becomes smaller to nanometer scale. Especially the ratio of surface to volume atoms, and the face center cubic (fcc) to body center cubic (bcc) structural transition of Fe are expected to play crucial roles in manipulation of magnetisom for Fe nanostructures. Thus, in this report, Xe-buffer layer-assisted growth (BLAG) [17], Au(111) herringbone reconstruction surface, and annealing effect are combined to manipulate Fe growth on Au(111), in order to form well-ordered 2-D island arrays with different stacking heights and lateral sizes.

Manuscript received March 06, 2009. Current version published September 18, 2009. Corresponding author: C.-C. Kuo (e-mail: cckuo@mail.nsysu.edu.tw).

Color versions of one or more of the figures in this paper are available online at http://ieeexplore.ieee.org.

Digital Object Identifier 10.1109/TMAG.2009.2025183

II. Experiment

The experiment was carried out in a multifunctional ultrahigh vacuum (UHV) chamber with base pressure $= 4 \times 10^{-11}$ mbar. All the sample preparation and characterization were performed *in situ*. After cycles of 500 eV Ar^+ sputtering and annealing, clean Au(111) surface with herringbone structure was prepared. To grow Fe nanoparticles, Fe atoms evaporated by e-beam heating were deposited onto either the bare substrate or the substrate covered with Xe buffer layer. The deposition rate of Fe is $6–9 \times 10^{-4}$ ML/s. For the room-temperature (RT) growth, the substrate is controlled at 300 K. Xe BLAG was performed by Xe adsorption, and subsequent Fe deposition at 90 K. Then, the sample was annealed to 300 K for the desorption of Xe and formation of stable Fe islands. The grown samples were characterized by an UHV scanning tunneling microscope (STM) for further analysis on the morphology and crystalline structure.

III. Results and Discussion

A. RT-Grown Fe 2-D Islands

Fig. 1(a) exhibits the STM images of herringbone reconstruction of Au(111) surface. From the line profile, the corrugation of herringbone structure is about 0.1 Å and the periodicity is ~7.5 nm. Fig. 1(b)–(d) reveals RT growth of Fe on Au(111) herringbone surface. The 2-D islands with single atomic height gradually expand their size with increasing Fe coverage. The ordered arrangement of Fe islands is always the same, while up to 0.35 ML, only less than 1% of the total area is covered by the second layer and a few islands start to coalesce with the nearby one.

Fig. 2 summarizes the statistics from STM images of n ML RT-grown Fe on Au(111). In Fig. 2(a), the island density is kept around 170 ± 10 per 100×100 nm^2 when below 0.4 ML.

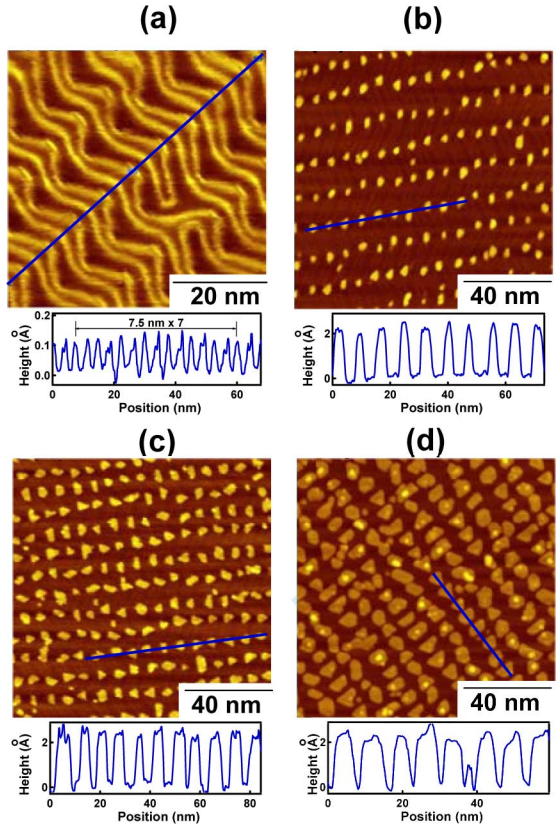

Fig. 1. STM images of (a) Au(111) herringbone structure, (b) 0.05-ML Fe, (c) 0.2-ML Fe, and (d) 0.35-ML Fe, with the line profiles in the bottom.

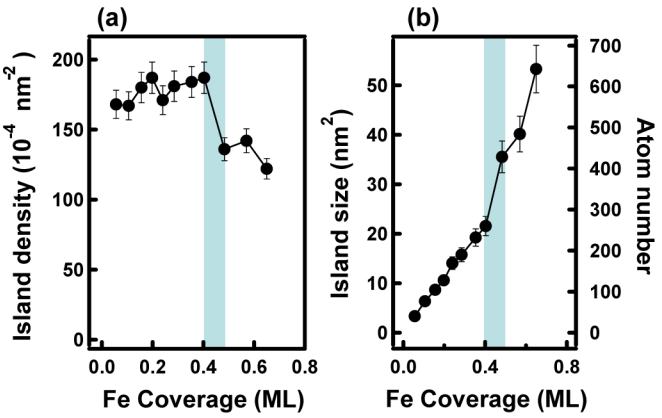

Fig. 2. Average Fe island density and size as functions of Fe coverage, analyzed from statistical results of STM images.

During 0.4–0.6 ML, the island density drops down to 120–130 per 100×100 nm^2, indicating the significant coalescence between nearby islands. In previous reports, Fe underwent pseudomorphic growth on Au(111) (below 3 ML). Based on the Fe total coverage and the island density, the average island size and atom numbers are calculated in Fig. 2(b). The island size gradually increases to $\sim$20 nm^2 (200–300 atoms) before 0.4 ML, and then drastically expands to 35–55 nm^2 (400–700 atoms) during 0.4–0.6 ML. These statistical values are crucial to the magnetic behavior and will be discussed later in the text.

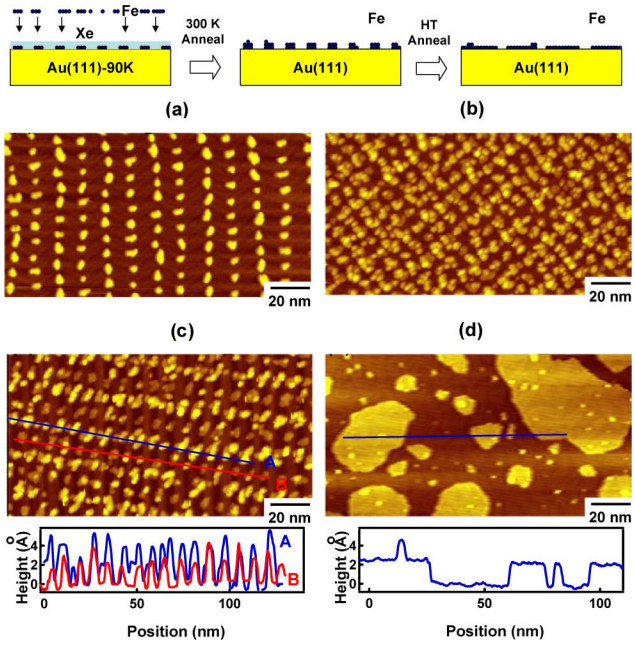

Fig. 3. Multistep growth of Fe on Au(111) herringbone structure. The figure exhibits the growth processes. (a)–(d) are STM images of 0.09-ML Fe nucleation seeds, subsequent growth of 0.27-ML Fe on Xe/0.09 ML seeds, 350-K annealing, and 600-K annealing.

B. Multistep Growth of Fe Islands

In addition to the above conventional RT-grown Fe 2-D islands, one might think about the possibility to stack the single-layer islands up to multilayers, with the same ordering and separation between islands. Unfortunately, further RT deposition of Fe results in layer-by-layer growth mode. Around 0.8–0.9 ML, the 2-D coalescence of the first Fe layer can be observed. Thus, in order to break the limitation of single atomic height in 2-D islands, the multistep growth is adopted, as shown in Fig. 3. Xe buffer layer, nucleation seeds, and thermal annealing are combined for the preparation. First, well-ordered nucleation seeds are prepared on Au(111), as shown in Fig. 3(a). Subsequently, 8 L (1 L $= 1 \times 10^{-6}$ torr $\times$ 1 s) Xe exposure is performed, and then Fe is deposited, at 90 K. After Fe deposition, annealing up to 300 K causes the Xe desorption and the morphology is exhibited in Fig. 3(b). During Xe desorption, Fe atoms gradually aggregate to form nanoislands with 1–2 atomic height, with their positions close to the previous nucleation sites. Rectangular lattice can be observed in the regular Fe island arrays.

Postannealing processes at 350 and 600 K are also performed and the corresponding STM images are shown in Fig. 3(c) and (d), respectively. Interestingly, 350-K annealing rearranges the Fe islands into two kinds of chains. As depicted in the line profiles of Fig. 3(c), one kind of island chain prefers bilayer islands (line profile A), while the other kind prefers single-layer islands (line profile B). Further 600-K annealing, as shown in Fig. 3(d), results in significant coalescence and large 2-D islands are observed. In short, thermal annealing can enhance the movement of small islands, leading to better ordering or large scale 2-D islands by properly choosing annealing temperature.

C. Magnetic Behavior

The well-ordered single-atomic-layer Fe islands actually provide us with a very standard and interesting system for the discussion of magnetic behavior in low-dimensional nanostructures. In the last decade, the phenomenological Néel-type model has been used successfully to describe the thickness-dependent spin-reorientation transition (SRT) in various thin film systems, while considering the contributions from surface and volume, which are the so-called surface anisotropy and volume anisotropy terms [18], [19]. Similarly, by assuming that the Fe 2-D islands are just like circular discs, one can consider the contributions from the edge atoms (MAE_e) and from the surface atoms (MAE_s). The total magnetic anisotropy energy (MAE) is written as $\mathrm{MAE} = \mathrm{MAE}_e \cdot 2\pi R + \mathrm{MAE}_s \cdot \pi R^2$, where $R =$ disc radius. Considering that the 2-D islands are all of single atomic height, ($\pi R^2 \cdot$ island number) must be proportional to the total Fe coverage t. Because the island number (= herringbone elbow number) is invariant before coalescence, we have $R^2 \propto t$, or $R \propto \sqrt{t}$. Thus, the MAE per atom (divided by πR^2) can be rewritten as

$$\mathrm{MAE} = E_e/\sqrt{t} + E_s. \tag{1}$$

In order to simplify the equation, after combining the coefficients, the contributions from edge (MAE_e) and surface (MAE_s) are renamed as E_e and E_s, respectively. Fig. 4(a) shows MAE measured by Ohresser *et al.* as well as the fitting curve by (1) [6]. Ohresser *et al.* performed the magnetic characterization and the thin film growth *in situ* by X-ray magnetic circular dichroism (XMCD) in an ultrahigh-vacuum chamber (5×10^{-11} mbar), which is very close to our experiment condition. Thus, one can expect that our and Ohresser *et al.*'s samples should reveal the similar physical properties, which indeed are confirmed by the consistence between our modeling analysis and their experimental data. The fitting describes the experimental results well (below 0.4 ML), with the following fitting parameters: edge contribution: $E_e = +0.48$ meV/atom, preferring in-plane magnetization; surface contribution: $E_s = -0.767$ meV/atom, preferring perpendicular magnetization. Thus, while increasing Fe coverage, the average size of 2-D islands increases and the SRT is induced from edge-dominated in-plane anisotropy to surface-dominated perpendicular anisotropy. For the higher coverage (above 0.4 ML), the studies by Ohresser *et al.* reveal the second SRT from perpendicular to in-plane again. Apparently, (1) is not enough to describe the second SRT and thus the shape MAE is included.

As already known, the islands are always of one atomic height with expanding lateral size, while increasing Fe coverage. The ratio of height (d) to radius (R): d/R is depicted in the right axis of Fig. 4(b) as a function of Fe coverage. Furthermore, Fig. 4(b) shows the calculated disc shape anisotropy according to the d/R values. The lower and higher dotted lines are calculated with low-spin ($m = 1.4\ \mu_B$) and high-spin ($m = 2.4\ \mu_B$) states [6]. In the previous report on n ML Fe/Au(111) by Ohresser *et al.*, the Fe spin moment underwent a transition from low spin to high spin at ~0.3 ML [6]. The black solid line in Fig. 4(b) indicates the real evolution of shape MAE, as considering the

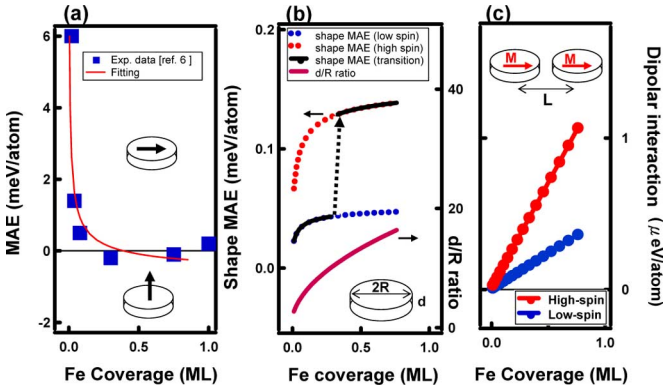

Fig. 4. (a) Measured MAE of Fe 2-D islands in [6] with the fitting curve of (1). (b) Calculated shape MAE and corresponding dimension ratio d/R of Fe discs based on the STM analysis results in Fig. 2. (c) Coupling energy of the nearby discs due to the dipolar interaction, as shown in (2).

transition. From the combination of Fig. 4(a) and (b), the contribution of edge atoms is insignificant during 0.4–1 ML, and the shape MAE gradually dominates the magnetic behavior and induces the second SRT back to in-plane due to the transition to high-spin state. From another point of view, even up to 1-ML Fe, there is still ~20% of Au(111) surface uncovered. Therefore, the effective surface area should be smaller than the expectation of (1). It implies that the surface contributing to perpendicular MAE is actually smaller than the expectation of (1). Thus, the second SRT transferring back to in-plane magnetization is promoted.

Besides the above discussion, the dipolar interaction between the nearby islands, preferring in-plane magnetization, might also influence the magnetic behavior. Considering the dipolar energy difference between the two cases of in-plane and perpendicular magnetization, we can get the MAE originating from island–island interaction, by simply calculating the magnetic dipole–dipole interaction energy [20]

$$E_{\mathrm{dipolar}} = (\mu_0/4\pi)3M^2/(L^3) \tag{2}$$

where M is the magnetization, and L is the interisland distance = 7.5 nm, just the same as the periodicity of herringbone structutre. As shown in Fig. 4(c), MAE (per atom) originating from island–island dipolar interaction is calculated by assuming that the magnetic moment is concentrated at the center of discs. From Bennett and Xu's report, the integration results of real condition are only 1–1.7 times the simplified calculation [20]. The E_{dipolar} is relatively much smaller than MAE in Fig. 4(b) and (c), and should not play any significant role.

IV. Summary

In summary, RT-grown Fe 2-D islands provides an ideal system for the understanding of the interrelation between dimensionality control and magnetism. Detailed morphology evolution of island size and arrangement is characterized by STM. Combining the statistical analysis of morphology, a phenomenological MAE model, as well as the shape MAE, the previously reported magnetic behavior of Fe 2-D island array can be described well. While increasing the Fe coverage, MAE is dominated by edge atoms, surface atoms, and then shape

MAE, sequentially. The multistep growth also indicates the chance for manipulating the growth of Fe islands into desired multilayer islands.

ACKNOWLEDGMENT

This work was supported by the National Science Council of Taiwan under Grants NSC 96-2112-M-003-015-MY3, NSC 96-2112-M-110-002, and NSC 97-2112-M-110-003-MY3.

REFERENCES

[1] F. M. Leibsle, S. S. Dhesi, S. Barrett, and A. Robinson, *Surf. Sci.*, vol. 317, pp. 309–320, 1994.
[2] H. Ellmer, V. Repain, M. Sotto, and S. Rousset, *Surf. Sci.*, vol. 511, pp. 183–189, 2002.
[3] K. Bromann, M. Giovannini, H. Brune, and K. Kern, *Eur. Phys. J. D*, vol. 9, pp. 25–28, 1999.
[4] H. Brune, M. Giovannini, K. Bromann, and K. Kern, *Nature*, vol. 394, pp. 451–453, 1998.
[5] J. A. Stroscio, D. T. Pierce, R. A. Dragoset, and P. N. First, *J. Vac. Sci. Technol. A*, vol. 10, pp. 1981–1985, 1992.
[6] P. Ohresser, N. B. Brookes, S. Padovani, F. Scheurer, and H. Bulou, *Phys. Rev. B, Condens. Matter*, vol. 64, 2001, 104429.
[7] J. Meyer, I. Baikie, E. Kopatzki, and R. Behm, *Surf. Sci.*, vol. 365, pp. L647–L651, 1996.
[8] N. A. Khan, *Christopher Matranga Surf. Sci.*, vol. 602, pp. 932–942, 2007.
[9] D. T. Dekadjevi, B. J. Hickey, and S. Brown, *Phys. Rev. B, Condens. Matter*, vol. 71, 2005, 054108.
[10] H. Bulou, F. Scheurer, P. Ohresser, A. Barbier, S. Stanescu, and C. Quiros, *Phys. Rev. B, Condens. Matter*, vol. 69, 2004, 155413.
[11] S. Rusponi, T. Cren, N. Weiss, M. Epple, P. Buluschek, L. Claude, and H. Brune, *Nature Mater.*, vol. 2, pp. 546–551, 2003.
[12] W. C. Lin, C. C. Kuo, M. F. Luo, K. J. Song, and M.-T. Lin, *Appl. Phys. Lett.*, vol. 86, 2005, 043105.
[13] M. F. Luo, C. I. Chiang, H. W. Shiu, S. D. Sartale, and C. C. Kuo, *Nanotechnology*, vol. 17, pp. 360–366, 2005.
[14] W. C. Lin, P. C. Huang, K. J. Song, and M.-T. Lin, *Appl. Phys. Lett.*, vol. 88, 2006, 153117.
[15] W. C. Lin, S. S. Wong, P. C. Huang, C. B. Wu, B. R. Xu, C. T. Chiang, H. Y. Yen, and M.-T. Lin, *Appl. Phys. Lett.*, vol. 89, 2006, 153111.
[16] C. C. Kuo, C. L. Chiu, W. C. Lin, and M.-T. Lin, *Surf. Sci.*, vol. 520, pp. 121–127, 2002.
[17] R. Skomski, J. Zhang, V. Sessi, J. Honolka, K. Kern, and A. Enders, *J. Appl. Phys.*, vol. 103, 2008, 07D519.
[18] W. C. Lin, B. Y. Wang, Y. W. Liao, K.-J. Song, and M.-T. Lin, *Phys. Rev. B, Condens. Matter*, vol. 71, 2005, 184413.
[19] M.-T. Lin, W. C. Lin, C. C. Kuo, and C. L. Chiu, *Phys. Rev. B, Condens. Matter*, vol. 62, pp. 14268–14272, 2000.
[20] A. J. Bennett and J. M. Xu, *Appl. Phys. Lett.*, vol. 82, pp. 2503–2505, 2003.